Journal of Theoretical Biology 347 (2014) 63–73

Contents lists available at ScienceDirect

Journal of Theoretical Biology

journal homepage: www.elsevier.com/locate/yjtbi

Modeling inoculum dose dependent patterns of acute virus infections

Yan Li [a], Andreas Handel [b,*]

[a] Institute of Bioinformatics, The University of Georgia, Athens, GA, USA
[b] Department of Epidemiology and Biostatistics, The University of Georgia, Athens, GA, USA

AUTHOR-HIGHLIGHTS

- Acute viral infections show consistent patterns of inoculum dose dependence.
- Most existing models fail to reproduce the observed inoculum dependent patterns.
- Models including innate and adaptive immunity can reproduce the observed patterns.

ARTICLE INFO

Article history:
Received 15 October 2013
Received in revised form
31 December 2013
Accepted 6 January 2014
Available online 15 January 2014

Keywords:
Within-host model
Immune response dynamics

ABSTRACT

Inoculum dose, i.e. the number of pathogens at the beginning of an infection, often affects key aspects of pathogen and immune response dynamics. These in turn determine clinically relevant outcomes, such as morbidity and mortality. Despite the general recognition that inoculum dose is an important component of infection outcomes, we currently do not understand its impact in much detail. This study is intended to start filling this knowledge gap by analyzing inoculum dependent patterns of viral load dynamics in acute infections. Using experimental data for adenovirus and infectious bronchitis virus infections as examples, we demonstrate inoculum dose dependent patterns of virus dynamics. We analyze the data with the help of mathematical models to investigate what mechanisms can reproduce the patterns observed in experimental data. We find that models including components of both the innate and adaptive immune response are needed to reproduce the patterns found in the data. We further analyze which types of innate or adaptive immune response models agree with observed data. One interesting finding is that only models for the adaptive immune response that contain growth terms partially independent of viral load can properly reproduce observed patterns. This agrees with the idea that an antigen-independent, programmed response is part of the adaptive response. Our analysis provides useful insights into the types of model structures that are required to properly reproduce observed virus dynamics for varying inoculum doses. We suggest that such models should be taken as basis for future models of acute viral infections.

1. Introduction

Inoculum dose, i.e. the number of pathogens at the beginning of an infection, can affect key aspects of pathogen dynamics following infection, such as the initial rate of pathogen growth, peak pathogen levels, time at which pathogen peak is reached, and total pathogen load (Prince et al., 1993; Ottolini et al., 1996; Liu et al., 2009; Ginsberg and Horsfall, 1952; Callison et al., 2006; Powell et al., 2006; Hughes et al., 2002; Legge and Braciale, 2005). Pathogen dynamics in turn affects the ensuing immune response (Powell et al., 2006; Legge and Braciale, 2005; Marois et al., 2012; Hatta et al., 2010). Pathogen dynamics and immune response together determine clinically relevant outcomes, such as morbidity and mortality (Goldberg et al., 1954; La Gruta et al., 2007; Gowthaman et al., 2010; Leggett et al., 2012; Moskophidis et al., 1995). Maybe surprisingly, despite the general recognition that inoculum dose is an important component of infection outcomes, we currently do not understand in any detail how and why changes in inoculum dose impact infection outcomes. While concepts such as the 50% infectious or lethal dose – which acknowledge the importance of inoculum – are commonly used (Blaser and Newman, 1982; Schmid-Hempel and Frank, 2007; Boon et al., 2009), little effort has been made to understand the impact of inoculum dose on infection outcomes in a systematic manner.

Mathematical models are well suited for the detailed analysis of infection dynamics and have contributed much to our understanding (e.g. Nowak and May, 2000; Perelson, 2002; Asquith and

* Corresponding author.
E-mail address: ahandel@uga.edu (A. Handel).

0022-5193/$ - see front matter © 2014 Elsevier Ltd. All rights reserved.
http://dx.doi.org/10.1016/j.jtbi.2014.01.008

Bangham, 2003; Antia et al., 2005). Previous models have been able to describe many important features of the dynamics of pathogens and the host response upon infection. At the same time, as we continue to better understand the within-host dynamics of many infectious diseases and obtain better data, model limitations are being realized. An ongoing process of model refinement ensures their ability to properly reproduce the observed data. One pattern often seen in a variety of different infections is a dependence of the pathogen and immune response dynamics on the inoculum dose. While a few recent models considered the role of the inoculum (Howey et al., 2009; Steinmeyer et al., 2010), a systematic understanding of the types of models needed to reproduce the inoculum dose dependent patterns that are observed in pathogen and immune response dynamics is lacking. This study is intended to fill this gap by analyzing existing models with regard to their ability to reproduce inoculum dependent patterns of viral load dynamics. We find that models including components of both the innate and adaptive immune response are needed to describe the patterns found in the data. We further show that only some of the ways in which the innate or adaptive immune response have been modeled in the past agree with observed data. Our analysis provides useful insights into the types of model structures that are required to properly reproduce observed virus dynamics for varying inoculum doses.

2. Methods

2.1. Basic infection dynamics model

We consider a range of different models to describe the dynamics of an acute viral infection. We describe the different model variants in Section 3. All of these model variations are extensions of the basic model for an acute virus infection (Beauchemin and Handel, 2011; Smith and Perelson, 2011), which is given by the following three differential equations:

$$\dot{U} = -bUV$$
$$\dot{I} = bUV - dI$$
$$\dot{V} = pI - cV \qquad \text{(B1)}$$

The model tracks the number of susceptible target cells, U, infected cells, I, and the number of infectious, free virions, V. The infection process is modeled through a mass-action term, bUV. Infected cells produce virus at rate p and die at rate d. Free virus can go on to infect new cells or is cleared from the system at rate c. For more details on this model and similar ones, see e.g. Beauchemin and Handel (2011) and Smith and Perelson (2011).

2.2. Estimating characteristic features of viral load dynamics

While the basic acute virus infection model given by (B1) can capture the observed viral load patterns described below, the model contains too many parameters and unknown initial conditions to allow estimation of all of them (Smith et al., 2010; Beauchemin and Handel, 2011). To prevent overfitting and to obtain more robust results, we therefore make use of a simpler, four parameter phenomenological equation, which was previously shown to fit viral load data from acute infections well (Holder and Beauchemin, 2011). The equation is given by

$$V(t) = \frac{2p_1}{\exp(-p_2(t-p_3)) + \exp(-p_4(t-p_3))} \qquad \text{(P1)}$$

where the p_i are the parameters that are being fit. We fit by minimizing the least squares difference between the logarithm of model and data. We then use the expression $V(t)$ for the viral load to determine the characteristic features as described in Section 3.

2.3. Model implementation

All models were implemented in R (R Development Core Team, 2012). The computer code is available from the authors on request.

3. Results

3.1. Characterization of inoculum dose dependent viral load patterns

Inoculum dose is known to impact the dynamics and outcome of many infectious diseases. For the present study, we focus on pathogen load during acute viral infections. As illustrative examples, we consider two previously published datasets; for adenovirus type 5 (ADV) infection of cotton rats (Prince et al., 1993) and infectious bronchitis virus (IBV) infection in chicken (Callison et al., 2006). Figs. 1 and 2 show viral load data for 3 different inoculum doses for the two infections. Similar inoculum dose dependent pathogen dynamics can be found throughout the literature for other host–pathogen systems (see e.g. Liu et al., 2009; Ottolini

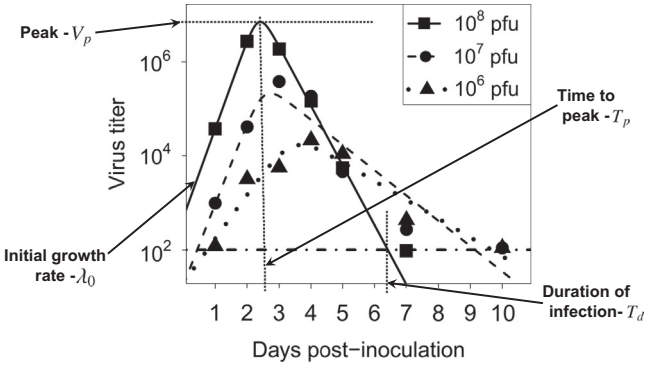

Fig. 1. Adenovirus titer for different inoculum doses. Symbols show experimentally determined viral load data for different inoculum doses for Adenovirus type 5 (ADV) infections of cotton rats. For details see Prince et al. (1993). The lines are obtained by fitting Eq. (P1) to the data. The dash-dotted horizontal line shows the limit of detection.

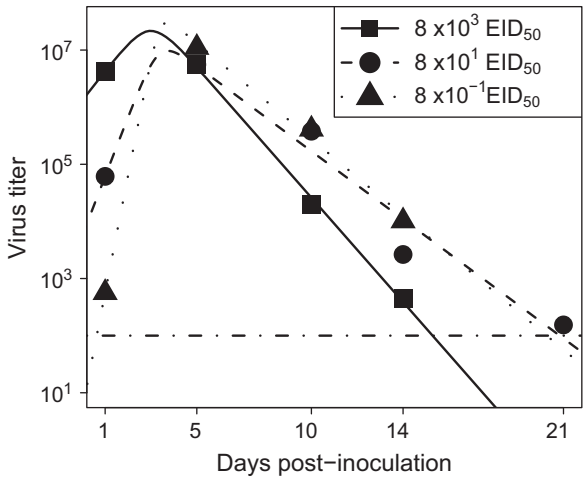

Fig. 2. Infectious bronchitis virus titer for different inoculum doses. Symbols show experimentally determined viral load data for different inoculum doses for infectious bronchitis virus (IBV) infections of chickens. For details see Callison et al. (2006). The lines are obtained by fitting Eq. (P1) to the data. The dash-dotted horizontal line shows the limit of detection.

et al., 1996, 2005; Ginsberg and Horsfall, 1952; Howey et al., 2009; Quan et al., 2004; Powell et al., 2006; Legge and Braciale, 2005).

It was previously shown that the viral load dynamics of acute viral infections can be well characterized by a few summary quantities (Smith et al., 2010; Holder and Beauchemin, 2011). Following these earlier studies, we define a suitable set of characteristic features that can fully describe the observed viral load dynamics. Specifically, we characterize the viral load curve by 4 summary features: (i) initial growth rate of virus, λ_0, defined as the initial slope of exponential growth; (ii) peak viral load, V_p (in log units); (iii) time of viral load peak, T_p; (iv) duration of infection T_d, defined as the time post infection at which viral titer drops below the limit of detection. Fig. 1 illustrates those four features.

Our main interest is in how these characteristic features depend on the inoculum dose. The symbols in Fig. 4 show these features for the two datasets as a function of inoculum dose. For ADV, one finds an increase in the initial virus growth rate and virus peak as inoculum dose increases, while time to peak and duration of infection decrease. For IBV, one sees a decrease in the initial growth rate as inoculum increases, the virus peak remains essentially constant and the time to peak and duration of infection decrease. The patterns seen for the ADV and IBV data are representative of patterns seen in other host–pathogen systems (Liu et al., 2009; Ottolini et al., 1996, 2005; Ginsberg and Horsfall, 1952; Howey et al., 2009; Quan et al., 2004; Powell et al., 2006; Legge and Braciale, 2005). In general, specifics of the pathogen, host, and inoculum dosing ranges determine the observed patterns, which might be different than those for ADV and IBV. Our goal in this study is not to match *every* possible inoculum-dependent pattern that might exist. Instead, we study how well current models can reproduce commonly observed patterns such as those seen for ADV and IBV and what kinds of mechanisms are needed to be able to match the observed data.

3.2. The basic acute infection model cannot reproduce inoculum dose dependent patterns

To analyze the ability of current models to reproduce the inoculum dose dependent patterns observed in the data, we start with the basic model (B1) for acute viral infections described in Section 2. Fig. 3 shows virus dynamics for 3 different inoculum doses. One sees that the virus peak and initial growth rate are inoculum dose independent, while time to peak and duration of infection show inoculum dose dependence.

For the simple model (B1), one can obtain analytical approximations for the characteristic features introduced in the previous section. At the beginning of the infection, one can make the approximation that the number of susceptible target cells is approximately constant, i.e. $U \approx U_0$. This reduces model (B1) to a linear model, which can be solved analytically (Nowak et al., 1997; Smith et al., 2010). One finds that viral load grows exponentially as $V(t) = V_0 e^{\lambda_0 t}$ where the growth rate is given by

$$\lambda_0 = \frac{\sqrt{(d-c)^2 + 4bpU_0} - d - c}{2}. \tag{B2}$$

With the approximation that the exponential growth of virus continues up to the peak, one immediately finds the time of virus peak as

$$T_p = \frac{1}{\lambda_0} \log\left[\frac{V_p}{V_0}\right]. \tag{B3}$$

The approximation of constant growth up to the peak is of course not completely accurate since close to the peak, growth slows down and is zero at the peak. However, the approximation is fairly accurate and further refinements do not change the result much

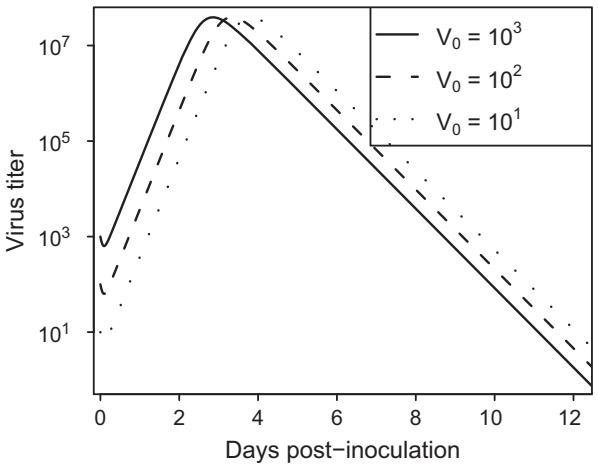

Fig. 3. Within-host virus dynamics obtained from model (B1) for different inoculum doses. Initial conditions are $U_0 = 10^7$, $I_0 = 0$ and V_0 as indicated. Values for model parameters are $b = 1 \times 10^{-7}$, $p = 100$, $d = 2$, $c = 10$. In all simulations, units of rate parameters are inverse days. Since we do not have parameter estimates for ADV and IBV, we chose parameter values similar to estimates for influenza (Beauchemin and Handel, 2011). The exact choice for the parameter values does not matter. The numbers should therefore be regarded as essentially arbitrary and simply chosen to obtain viral load dynamics that looks similar to that observed in the ADV and IBV data. Importantly, *no* choice of parameter values can produce inoculum dependent initial growth or peak of the viral load.

(Smith et al., 2010). An expression for the peak viral load, V_p, can be obtained as follows. First, we note that if we keep track of dead cells in our system, the number of cells remains constant, i.e. $N = U_0 = U + I + D$, where the dead cells are described by the equation $\dot{D} = dI$. The infected cells at the peak are then given by $I_p = U_0 - U_p - D_p$. We make another approximation, namely the often considered quasi-steady-state assumption for the virus dynamics, which is often reasonable since the virus dynamics tends to occur on a faster time-scale compared to the infected cell dynamics (Borghans et al., 1996; Segel and Slemrod, 1989). This allows us to express viral load in terms of infected cells, $V(t) \approx pI(t)/c$ and therefore $V_p \approx (c/p)(U_0 - U_p - D_p)$. It also allows us to write the equation for the dead cells as $\dot{D}(t) = dI(t) \approx dcV(t)/p = dcV_0 e^{\lambda_0 t}/p$. Integrating to the peak leads to $D_p = (cd/p\lambda_0)(V_p - V_0)$. Lastly, for our model, the number of uninfected cells at the peak, U_p, only depends on the reproductive number, R, which is given by $R = (bpU)/(cd)$ (Baccam et al., 2006; Beauchemin et al., 2008). At the peak, $R = 1$ by definition (Heffernan et al., 2005; Heesterbeek, 2002), which gives $U_p = (cd)/(bp)$. Putting it all together, we find that the peak is approximately given by

$$V_p = \frac{\lambda_0}{(\lambda_0 + d)}\left(\frac{p}{c}U_0 - \frac{d}{b} + \frac{dV_0}{\lambda_0}\right). \tag{B4}$$

While this suggests that the virus peak depends on V_0, inoculum dose has in fact almost no impact on virus peak. This can be seen by noticing that for almost any biologically relevant situation, $V_p \gg V_0$, and therefore $D_p \approx (cd/p\lambda_0)V_p$, leading to $V_p \approx (bpU_0 - dc)\lambda_0/bc(d + \lambda_0)$, which is independent of V_0.

Finally, we can obtain an approximation for the duration of the infection by realizing that shortly after the peak, most uninfected cells are gone, and the dynamics of the infected cells can be approximated as $\dot{I} = -dI$, i.e. exponential decay at rate d. Because of our quasi-steady state approximation, the same decay rate applies to the viral load. With this exponential decline, one finds that the duration of infection is approximately given by

$$T_d = T_p + \frac{\log(V_p/V_d)}{d}, \tag{B5}$$

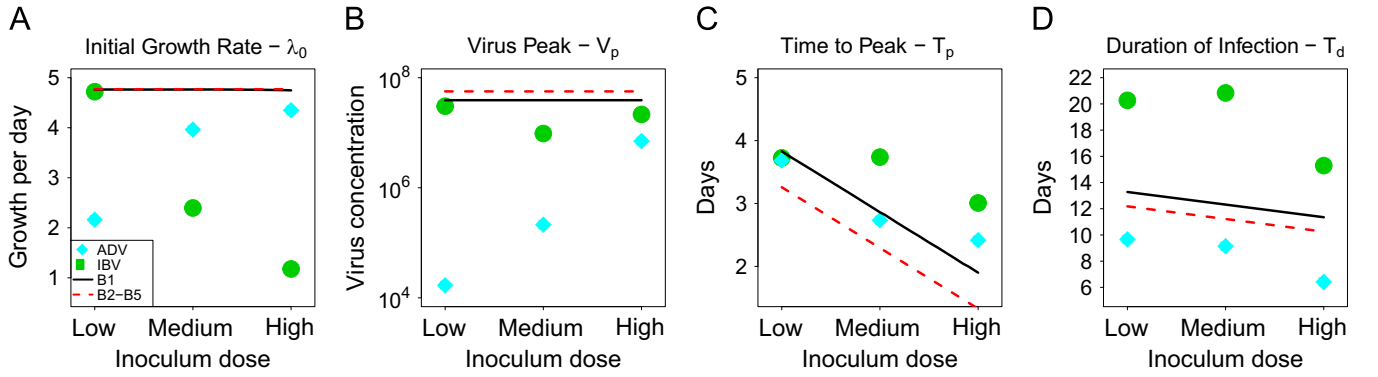

Fig. 4. Characteristic features described in Fig. 1 as a function of inoculum dose. Symbols show these features for the two datasets, determined by fitting Eq. (P1) to the data and then extracting the characteristic features from the smooth curve for $V(t)$. The lines show results obtained through simulation of the basic model (B1) (solid black line) or the analytical approximations (B2)–(B5) (dashed red line) using parameter values as given in Fig. 3 caption. Note that the two experiments are different host–pathogen systems, with different experimental assays used to measure virus load (pfu and EID_{50}). Inoculum doses in the two datasets are therefore not comparable, and also do not directly map to our model units of infectious virions. Since our focus is on the overall patterns and not quantitative agreement, and to allow presentation of data and model in an easy way, we categorized the experimental inoculum doses as low, medium and high. These values span 2 orders of magnitude for ADV and 4 orders for IBV. Theoretical results are obtained using inoculum doses in the range of 10^1–10^5 spanning 4 orders of magnitude. The inoculum dose dependent patterns we focus on are not affected by changes in the range. (For interpretation of the references to color in this figure caption, the reader is referred to the web version of this paper.)

where V_d is the limit of virus detection, which we assume to correspond to the end of the infection. Since as just explained, the virus peak is barely influenced by inoculum dose, it follows that the duration of infection has the same inoculum dependence as the time to peak.

Fig. 4 shows inoculum dose dependent patterns of virus growth rate, peak, time to peak and duration of infection; both for the analytical approximations (B2)–(B5) and for numerical simulations from the model (B1). The analytical approximations and model simulations agree reasonably well. We also find that the model cannot replicate the patterns observed in the data. Specifically, the change in the growth rate for ADV and IBV, and increase in the virus peak for ADV are not reproduced by the model. In the following sections, we analyze model variants and study their ability to better reproduce the observed inoculum dependent patterns. We focus on models that include different components of the immune response, both because those kinds of models are very common and because of their obvious biological relevance.

3.3. Models that include an innate immune response

Upon infection, the innate immune response acts as the first line of host defense and is crucial for orchestrating the full host response (Murphy, 2012). One can broadly divide the innate response into cellular and non-cellular, the latter being comprised of cytokines and other chemokines. Of course, those different components interact with each other, but they still have their distinct features and modes of action, and are usually modeled in distinct ways. We therefore consider them separately in the next two sections.

3.3.1. Cytokine based innate immune response

Different types of cytokines play an important role against acute viral infections (Murphy, 2012; Tamura and Kurata, 2004). Some of the most prominent ones are the interferons, especially type I interferon (IFN) (Randall and Goodbourn, 2008; Garcia-Sastre, 2002; Welsh et al., 2012). Because of its importance, IFN has been included in a number of models for acute viral infections, most notably models that describe influenza infection dynamics (Handel et al., 2010; Baccam et al., 2006; Saenz et al., 2010; Pawelek et al., 2012; Hancioglu et al., 2007; Dobrovolny et al., 2013; Canini and Carrat, 2011; Reperant et al., 2012). It is generally accepted that type 1 IFN is produced in response to infection of cells, either directly by the infected cells or by other nearby cells who "sense" that an infection is ongoing. This is usually modeled by assuming induction of IFN proportional to infected cells or proportional to viral load. The two formulations produce the same results with regard to inoculum dose dependence (not shown), we therefore only consider IFN induction proportional to infected cells. Another model variant with a delay for the activation in IFN (Mitchell et al., 2011; Baccam et al., 2006) also does not change the inoculum dose dependent patterns presented below (not shown).

While the dynamics of IFN is modeled very similar in most studies, the effect of IFN is being implemented in varied ways, corresponding to the biological finding that IFN has multiple modes of action. It is generally understood that IFN can induce an antiviral state in either uninfected or infected cells (Randall and Goodbourn, 2008; Tamura and Kurata, 2004; Garcia-Sastre, 2002). However, it is less clear how exactly this antiviral state should be described. One possibility is that IFN reduces virus production in already infected cells. The equations for a model of IFN dynamics and such a mode of action is given by (Baccam et al., 2006; Handel et al., 2010)

$$\dot{F} = gI - \delta_1 F$$
$$\dot{V} = \frac{p}{1+k_1 F} I - cV. \qquad \text{(F1)}$$

The rate of IFN induction is given by g, δ_1 describes the removal of IFN from the system, and k_1 represents the strength of reduction in virus production due to IFN. Note that here and in the following, we only display those equations that change from the base model. For any equation not shown explicitly, the base model equations (B1) apply. We also studied an alternative model for which IFN reduces infection rate b instead of virus production rate p (Handel et al., 2010). Such a model variant did not lead to any different results (not shown).

The equation describing IFN dynamics can be extended by explicitly including a term for absorption of IFN into cells (Bocharov and Romanyukha, 1994; Hancioglu et al., 2007), which gives

$$\dot{F} = gI - \delta_2 F - k_2 FI$$
$$\dot{V} = \frac{p}{1+k_1 F} I - cV, \qquad \text{(F2)}$$

where the term $k_2 FI$ describes the absorption of IFN into infected cells, while δ_2 describes removal of IFN by all other mechanisms.

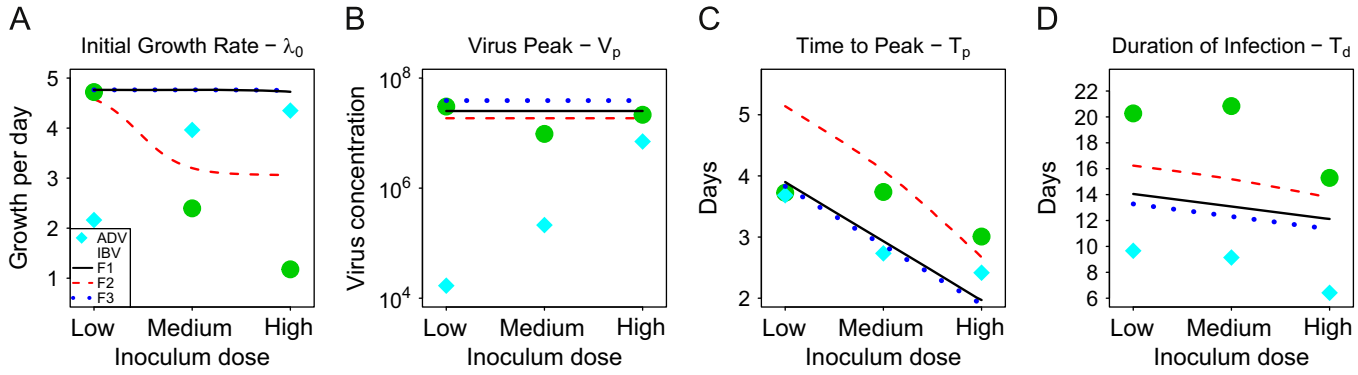

Fig. 5. Characteristic features described in Fig. 1 as a function of inoculum dose for different IFN immune response models. Units of all rate parameters are inverse days, parameter and initial condition values are as follows. For model (F1) (solid black line): $g=10^3$, $\delta_1=10^3$, $k_1=10^{-7}$, $F_0=1$. For model (F2) (dashed red line): $g=10^3$, $\delta_2=10^2$, $k_1=10^{-3}$, $k_2=2$, $F_0=1$. For model (F3) (dotted blue line): $g=10^3$, $\delta_2=10^2$, $k_3=10^3$, $k_4=10^{-3}$, $F_0=1$. All other parameter values as given in caption of Fig. 3. Note that choices of parameter values here and in all following figures are not meant to match the biology of any specific host-pathogen system. Instead, we chose essentially arbitrary values to show the types of inoculum dependent patterns that the different models are able to produce. (For interpretation of the references to color in this figure caption, the reader is referred to the web version of this paper.)

Another way the action of IFN has been modeled is by assuming that IFN mainly enters uninfected cells and renders them resistant to infection, which can be described by adding a term of IFN-based removal of uninfected cells into the model (Saenz et al., 2010; Pawelek et al., 2012; Reperant et al., 2012), leading to

$$\dot{F} = gI - \delta_2 F - k_3 FU$$
$$\dot{U} = -bUV - k_4 FU. \qquad \text{(F3)}$$

Fig. 5 shows how these different IFN models behave with regard to the inoculum dose dependent characteristic features we introduced earlier. Model (F1) has no effect on the growth rate as inoculum dose changes (solid black line). While IFN production increases with inoculum dose, it leads to directly proportional IFN mediated reduction in virus production, which in turn slows down further IFN production. The overall result of this tight feedback loop between IFN and viral load leads to the observed inoculum independent growth dynamics – no matter how model parameters are chosen. For model (F2), this tight feedback loop is broken. The additional absorption term (k_2FI) leads to IFN dynamics that saturates at a maximum level, independent of inoculum dose. This maximum IFN level is reached faster for higher inoculum doses, leading to a reduction in the initial growth rate (dashed red line). While model (F3) also includes an absorption term, this term describes absorption into uninfected cells. Since the number of uninfected cells is initially mostly constant and independent of inoculum dose, this model does not impact the initial growth rate (dotted blue line). None of the models lead to inoculum dependence for the virus peak. This would require models that have a strong virus (antigen) independent component, as we will explain in more detail below.

Note that while the results shown in Fig. 5 and subsequent figures are for specific parameter settings whose values are essentially arbitrary and not based on the biology of any particular host–pathogen system, we checked that these are general results. Many other parameter value combinations will produce the same overall patterns in the models. Obviously, parameter values can be chosen for which these patterns are not observed (e.g. parameter values that "turn off" the immune responses). The main point we focus on is if a given model can produce certain inoculum dependent patterns, at least for some parameter value choices.

To summarize this section, currently existing models that include a cytokine innate response – most often considered to be IFN – can only reproduce decreasing initial growth rates as observed for instance in the IBV dataset. Different models are needed to reproduce the increase in the initial growth rate and virus peak seen for instance for the ADV data.

3.3.2. *Cell based innate immune response*

Macrophages, neutrophils, dendritic cells, NK cells and other cell types constitute the cellular arm of the innate response (Murphy, 2012). These cells serve as first-line defenders against invading pathogens and also play vital roles in triggering the adaptive response. These innate cells have been considered for some acute viral infection models (Bocharov and Romanyukha, 1994; Canini and Carrat, 2011; Pawelek et al., 2012). Several other studies of non-viral or generic pathogens have also considered cellular innate responses (Antia and Koella, 1994; Pilyugin and Antia, 2000; Smith et al., 2011; Kochin et al., 2010; Handel et al., 2009). Macrophages are frequently modeled, we therefore focus on those cells, while noting that the same types of equations will equally apply to other types of innate cellular responses, e.g. NK cells or neutrophils. In the absence of an infection, macrophages are produced and die at relatively fixed rates. An infection leads to increased production or recruitment, up to some maximum level. The action of macrophages is usually modeled as killing of the pathogen in a mass-action manner (Antia and Koella, 1994; Pilyugin and Antia, 2000). For viral infections, this likely involves killing of infected cells (Herold et al., 2008; Höegner et al., 2013). These biological details can be described by a model of the form (Antia and Koella, 1994)

$$\dot{M} = s + gV(M^* - M) - \delta M$$
$$\dot{I} = bUV - dI - k_M MI, \qquad \text{(M1)}$$

where s is a basic rate of macrophage production, g is the rate of increase of production that depends on pathogen load and levels off as M reaches some maximum value, M^*, δ is the death rate and k_M is the rate of killing of infected cells by macrophages. An extension of this model to account for the fact that it takes time for a macrophage to kill a parasite or infected cell was introduced in Pilyugin and Antia (2000). The authors showed that a model that includes explicit compartments for free macrophages and those bound to cells while killing could be simplified through a quasi-steady-state approximation to yield a simpler, two-equation model given by

$$\dot{M} = (s + gV)(M^* - M - \alpha k_M MI) - \delta M$$
$$\dot{I} = bUV - dI - k_M MI. \qquad \text{(M2)}$$

Fig. 6 shows results for these cellular innate response models. We find that model (M1) (solid black line) can produce a decline in the

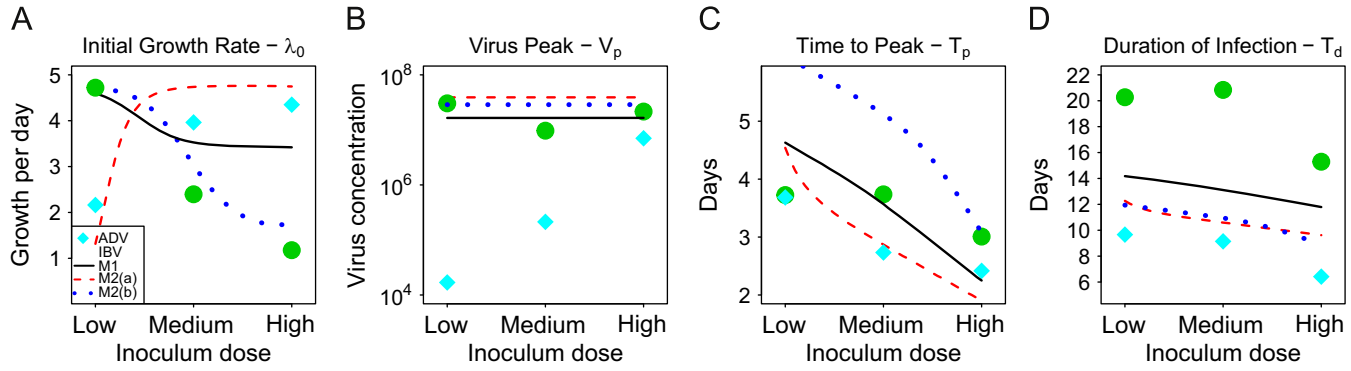

Fig. 6. Characteristic features described in Fig. 1 as a function of inoculum dose for different cellular innate immune response models. Units of all rate parameters are inverse days, parameter and initial condition values are as follows. For model (M1) (solid black line): $s=10^3$, g=0.1, $M^*=10^4$, $\delta=10$, $k_M=2\times10^{-4}$, $M_0=s/\delta$. For model (M2)(a) (dashed red line): $s=10^2$, $g=10^{-5}$, $M^*=10^4$, $\delta=10$, $\alpha=10^3$, $k_M=10^{-3}$, $M_0=(sM^*)/(s+\delta)$. For model (M2)(b) (dotted blue line): $s=10^{-2}$, $g=10^{-2}$, $M^*=10^4$, $\delta=10$, $\alpha=10^{-2}$, $k_M=5\times10^{-4}$, $M_0=(sM^*)/(s+\delta)$. All other parameter values as given in caption of Fig. 3. (For interpretation of the references to color in this figure caption, the reader is referred to the web version of this paper.)

initial growth rate as inoculum dose increases. The mechanism by which this happens is very similar to that for the IFN model (F2) discussed in the previous section. For model (M1), macrophage levels saturate at some upper level, depending on the value of M^* and independent of viral load. For a higher inoculum dose, the macrophages reach this maximum level faster, leading to reduced initial growth rate of the virus. A variant of model M1 with growth term $gVM(M^*-M)$ can also produce this pattern (not shown).

Since model (M2) is an extension of model (M1), it can produce the same pattern as model (M1) (dotted blue line). In addition, for different choices of parameter values, model (M2) can produce an increase in the virus growth rate as inoculum dose increases, as observed for the ADV data (dashed red line). This pattern is observed if the initial number of macrophages and time to kill infected cells are both reasonably large. For such a scenario, as the inoculum dose increases, more of the initially present macrophages become "tied up" killing infected cells, allowing the viral load to grow faster initially, until the infection-induced production or recruitment of macrophages dominates. This scenario is biologically reasonable only if there is a time window after killing during which macrophages need to recharge. It is not well known if this indeed occurs. Neither model leads to a change in the virus peak level as inoculum dose changes. For this to happen, immune response growth independent of viral load is needed, as we will discuss further below.

To summarize this section, models including a cellular innate response (being represented by macrophages in our examples) can, under certain circumstances, reproduce the pattern of either increased or decreased initial viral growth rate as inoculum dose increases. However, because of the feedback loops between virus growth and immune response growth, these models cannot reproduce changes in the virus peak with increasing inoculum dose, as for instance observed for the ADV data.

3.4. Models that include an adaptive immune response

While the innate immune response dominates at the beginning of an acute viral infection, the adaptive response is usually instrumental in bringing the virus under control and clearing it (Enquist et al., 1999; Braciale et al., 2012). The importance of the adaptive response for virus control and clearance is seen in experiments with immunocompromised animals or in natural infections of immunocompromised human hosts (Dobrovolny et al., 2013). In the following sections, we will explore models for two of the main components of the adaptive response, namely $CD8^+$ T cells and B cells/antibodies (Ahmed and Gray, 1996). We will analyze how models for these components affect the inoculum dose dependent patterns observed in the data.

3.4.1. $CD8^+$ T cell based adaptive immune response

Because $CD8^+$ T cells are important for the control of primary infections and protection through immunological memory against subsequent infections, and because it is possible to obtain reliable quantitative experimental data, these cells have received a large amount of attention, both experimentally and in modeling studies. The action of the $CD8^+$ T cells is to kill infected cells (Elemans et al., 2012), which is usually modeled through a mass-action killing term added to the infected cell equation. Several recent studies have shown that this modeling assumption fits available data fairly well (Regoes et al., 2007a,b; Yate et al., 2007; Ganusov et al., 2011). The detailed dynamics of $CD8^+$ T cells are still not fully understood (Andersen et al., 2006; Harty and Badovinac, 2008; Yewdell, 2010). A range of simplified models meant to capture the essential features of $CD8^+$ T cell dynamics have been developed (Wodarz, 2007). The first type of model employed to describe that $CD8^+$ T cell dynamics was equivalent to a predator–prey model frequently used in ecology (Nowak and May, 2000; Wodarz, 2007). $CD8^+$ T cells were assumed to grow proportional to pathogen load and die at a fixed rate. Such a predator–prey model for $CD8^+$ T cell dynamics, combined with mass-action killing of infected cells, can be written as

$$\dot{C}=r_1CV-\delta_CC$$
$$\dot{I}=bUV-dI-k_CIC, \qquad \text{(C1)}$$

here r_1 is a parameter describing the growth of activated $CD8^+$ T cells, δ_C is their rate of death and k_C their rate of killing infected cells. Models that assume activation of $CD8^+$ T cells proportional to infected cells (r_1CI) instead of viral load lead to similar results and we therefore do not further consider them. One problem with the basic predator–prey model is that it suggests increasing growth of $CD8^+$ T cells without bound as viral load increases, which is biologically unreasonable. Further, T cell activation and expansion involves multiple stages, some of which have been shown to depend on virus (antigen) load and some of which do not (Wong and Pamer, 2001; van Stipdonk et al., 2001; Kaech and Ahmed, 2001; Antia et al., 2003; Handel and Antia, 2008). Alternative models that lead to viral load independent growth as virus reaches high levels were subsequently used (De Boer and Perelson, 1995, 1998; Antia et al., 1996; Heffernan and Keeling, 2008), leading to models of the form

$$\dot{C}=\frac{r_2CV}{V+s_1}-\delta_CC$$

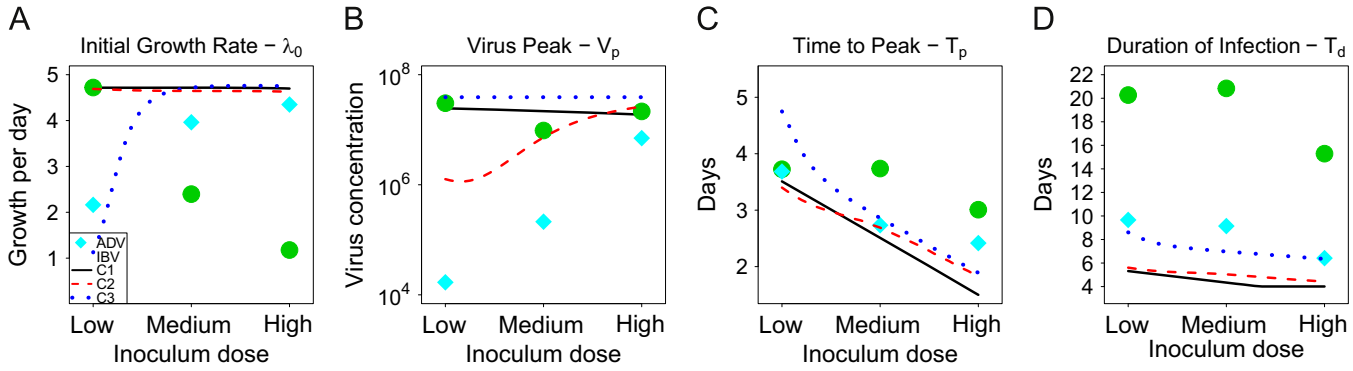

Fig. 7. Characteristic features described in Fig. 1 as a function of inoculum dose for different CD8$^+$ T cell models. Units of all rate parameters are inverse days, parameter and initial condition values are as follows. For model (C1) (solid black line), $r_1 = 10^{-6}$, $\delta_C = 1$, k_C=0.1, $C_0 = 1$. For model (C2) (dashed red line), r_2=2.5, $\delta_C = 1$, $s_1 = 10$, k_C=0.1, $C_0 = 1$. For model (C3) (dotted blue line), r_2=2.5, $\delta_C = 1$, $s_1 = 10$, $s_2 = 1$, k_C=0.1, $C_0 = 100$. All other parameter values as given in caption of Fig. 3. (For interpretation of the references to color in this figure caption, the reader is referred to the web version of this paper.)

$$\dot{I} = bUV - dI - k_C IC, \tag{C2}$$

where s_1 determines the level of virus at which growth becomes virus independent and r_2 determines the rate of growth. Another model variant takes into account the fact that it takes CD8$^+$ T cells time to kill infected cells, during which they cannot kill other cells (Pilyugin and Antia, 2000; Handel et al., 2009; Yates et al., 2011) – in close analogy to the macrophage model (M2) discussed above. This can for instance be written as

$$\dot{C} = \frac{r_2 CV}{V + s_1} - \delta_C C$$
$$\dot{I} = bUV - dI - \frac{k_C IC}{I + s_2}, \tag{C3}$$

where s_2 determines at which level of infected cells T cell killing saturates.

In Fig. 7, we show how these different CD8$^+$ T cell models affect the inoculum dose dependent virus patterns. Model (C1) does not show any inoculum dependence for virus growth or peak. In contrast, model (C2) can – for certain choices of parameter values – reproduce the inoculum dependent pattern of increase in the virus peak. The reason for this is that the saturation term allows the immune response to become largely independent of virus for high enough viral load. This means that the tight feedback loop between virus and immune response growth that was present for the innate response models we discussed above does not exist anymore. Instead, the strength of the immune response growth is largely independent of viral load. The time at which the immune response reaches high enough levels to bring the infection under control now depends little on viral load but instead on time since infection started. For a larger inoculum dose, the virus can reach higher levels before it is brought under control, compared to a lower inoculum dose.

CD8$^+$ T cell model (C3) shows – perhaps not surprisingly – a pattern similar to that found for the equivalent macrophage model, (M2). For certain parameter choices, this model leads to an inoculum dependent initial growth rate. The reason for this is that the addition of the expression $I + s_2$ in the killing term leads to saturated killing as the initial viral load, and therefore the infected cell numbers, increases. This in turn leads to an increase in the growth rate. The effect of the T cells on the initial growth rate is only observed if there are a large number of T cells at the beginning of the infection (C_0 relatively large), similar to the macrophage scenario described above. A large number of T cells are likely to be present if there is pre-existing immunity. In a naive host with few pathogen-specific T cells, the T cell dynamics is too slow to affect the initial growth rate. However, model (C3) does not affect the virus peak, in essence because the two saturation terms in both the T cell dynamics and killing cancel each other. If one chooses parameter values such that the saturation for the infected cell term becomes negligible (i.e. s_2 small), the model can produce virus peak pattern similar to model (C1). However for such parameter settings, the inoculum dependence of the growth rate disappears.

In addition to the models just discussed, we also analyzed a model with T cell growth that saturates at high T cell numbers (De Boer and Perelson, 1994; Wodarz, 2007), which did not lead to inoculum dependence. We further considered an extension of model (C2) that explicitly included an equation for the native CD8$^+$ T cells compartment (De Boer, 2007). This leads to the same results as those found with model (C2).

To summarize this section, we find that an antigen-independent component for T cell growth, together with mass-action killing captures the observed inoculum dependence for the ADV virus peak, and that a model that accounts for the fact that T cells need time to kill infected cells can influence the initial growth rate.

3.4.2. *B cell and antibody based adaptive immune response*

B cells, and the antibodies they produce, are the other main components of the adaptive immune response (Murphy, 2012). Upon infection, B cells are activated and subsequently undergo replication and produce pathogen-specific antibodies. Antibodies bind to virus and neutralize it (i.e. render it non-infectious). This can be modeled through a mass-action clearance term added to the equation describing infectious virus particles. While the detailed mechanisms of B cell and T cell activation differ, they have often been modeled with the same simplified equations containing activation and proliferation terms (Bocharov and Romanyukha, 1994; Hancioglu et al., 2007; Lee et al., 2008). Therefore, models of T cell dynamics described in the previous section have also been used for B cells. Here, we focus on a few previously used model alternatives that we have not yet considered. One recent model describing activation of B cells followed by clonal expansion can be written as (Handel et al., 2010)

$$\dot{B} = f_1 V + r_1 B$$
$$\dot{V} = pI - cV - k_B VB. \tag{A1}$$

The term $f_1 V$ describes antigen (virus) dependent activation, followed by antigen independent exponential growth through clonal expansion at rate r_1. This model ignores the contraction phase of B cells and can therefore only describe acute infections. The model further assumes that the equation for B cell dynamics also describes the dynamics of antibodies (i.e. it makes an implicit quasi-steady state assumption for the antibody dynamics).

Therefore, in this model B cells remove free infectious virus at rate k_B. More detailed models include an additional equation describing antibody production and removal (Lee et al., 2008; Bocharov and Romanyukha, 1994; Hancioglu et al., 2007; Vickers et al., 2009). One way to write an alternative, more detailed model is as follows:

$$\begin{aligned}\dot{B} &= f_2 BV + r_2(B^* - B)\\ \dot{A} &= r_a B - \omega k_A VA - d_a A\\ \dot{V} &= pI - cV - k_A VA,\end{aligned} \tag{A2}$$

where B cells are activated by recognizing virus antigen at rate f_2 and expand at rate r_2, saturating at a maximum value B^*. Activated B cells produce antibodies at rate r_a. Antibodies are removed from the system either through binding to virus at rate ωk_A (where ω represents the number of antibodies needed to neutralize a virion) or through other mechanisms at rate d_a. The action of antibodies on virus is modeled by the mass-action term k_{AVA}. One can include even further details, such as the plasma cell state of B cells as an explicit equation (Bocharov and Romanyukha, 1994; Hancioglu et al., 2007; Lee et al., 2008). This tends to introduce a time delay (Reperant et al., 2012; Perelson et al., 1976) but does not alter the inoculum dependent aspects of the dynamics.

Fig. 8 shows results for the different B cell and antibody models. For model (A1), one observes that if the antigen dependent component (the term $f_1 V$) is dominant, B cells are not able to impact virus peak (solid black line). However, if the antigen independent component dominates (the term $r_1 B$), B cells essentially grow exponentially at a constant rate independent of pathogen load (Handel et al., 2007, 2013) and can therefore influence the virus peak (red dashed line), akin to what was discussed for T cells above. Model (A2) has a constant influx term of B cells ($r_2 B^*$), and therefore constant production of antibodies in the absence of an infection. There is no virus independent *growth* component and the model can therefore not influence the virus peak pattern. However, this model can lead to increased initial virus growth as the inoculum dose increases (dash-dotted magenta line). This only happens if the background rate of antibodies in the absence of an infection is high (e.g. due to pre-existing immunity). In such a case, upon infection, antibodies are being "soaked up" by binding to virus (through the absorption term $-\omega k_A VA$). For a low virus inoculum, only a small fraction of the pre-existing antibodies are removed in this manner. Once inoculum increases, the initially present antibodies are immediately removed through binding to virus, allowing the remaining virus to grow at a faster rate until enough B cells are produced to replenish the pool of antibodies. This leads to an increase in the initial growth rate with increasing inoculum dose, very much like discussed above for the equivalent macrophage and T cell models.

To summarize this section, the B cell and antibody models can reproduce inoculum dependent patterns of growth for the initial growth rate or virus peak for certain scenarios, however they cannot impact both quantities simultaneously.

3.5. Models that can reproduce inoculum dependent patterns

In the preceding sections, we discussed a variety of models for components of the innate and adaptive immune responses and studied what kinds of mechanisms and model formulations can reproduce inoculum dependent viral load patterns observed in experimental data. We found that no individual immune response component or model is sufficient to capture all of the patterns, but combinations should be able to achieve this. We illustrate in Fig. 9 two such combination models, one that can reproduce the pattern seen in the ADV data and one that can reproduce the IBV pattern. While the impact of different components of the immune response on virus dynamics is not well known for either one of our infection systems (ADV in cotton rats or IBV in chickens), for ADV it was shown that macrophages respond to the infection (Prince et al., 1993; Nazir and Metcalf, 2005), and it was suggested that a T cell based response was important in the later part of the infection (Prince et al., 1993). We therefore used a combination of macrophage innate response model (M2) with T cell model (C2) for ADV. For IBV, cytokines such as IFN and B cell/antibodies are important components of the immune response (Cavanagh, 2007; Cook et al., 2012). We therefore used a combination of the cytokine innate response model (F2) with the B cell/antibody model (A1) for IBV. We want to emphasize that additional components of the immune response are also likely important in both infections. The choice of models should therefore mainly be understood as a "proof of concept", showing how combinations of innate and adaptive models can reproduce the observed inoculum dependent patterns seen in the data. Fig. 9 shows decent agreement. Improvements are likely possible through further tweaking of parameters or more rigorous fitting to the data. However, this is not our focus here, we only want to show that the models are able to capture the overall patterns seen in the data.

4. Discussion

Mathematical models have been successfully used for several decades to study and analyze the dynamics of virus infections.

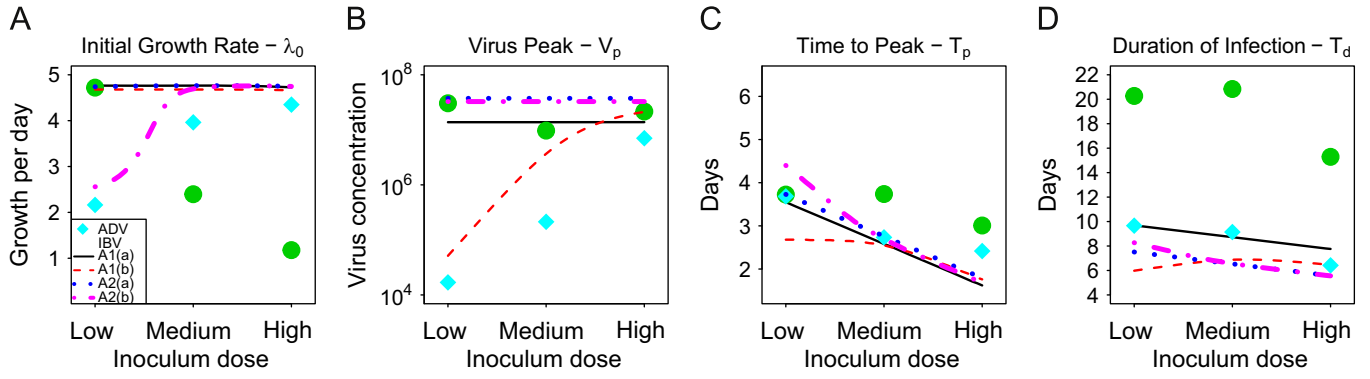

Fig. 8. Characteristic features described in Fig. 1 as a function of inoculum dose for different B cell and antibody models. Units of all rate parameters are inverse days, parameter and initial condition values are as follows. For model (A1)(a) (solid black line), $f_1 = 10^2$, $r_1 = 1$, $k_B = 10^{-8}$, $B_0 = 1$. For model (A1)(b) (dashed red line), $f_1 = 10^{-6}$, $r_1 = 2$, k_B=0.1, $B_0 = 1$. For model (A2)(a) (dotted blue line), $f_2 = 10^{-6}$, $r_2 = 1$, $B^* = 10^{-2}$, $r_a = 10^5$, $d_a = 100$, $\omega = 10^2$, k_A=0.01, $B_0 = B^*$ and $A_0 = r_a B^*/d_a$. For model (A2)(b) (dash-dotted magenta line), all parameters values are kept as in model (A2)(a) except $B^* = 1$, which alters the initial condition values B_0 and A_0. All other parameter values as given in caption of Fig. 3. (For interpretation of the references to color in this figure caption, the reader is referred to the web version of this paper.)

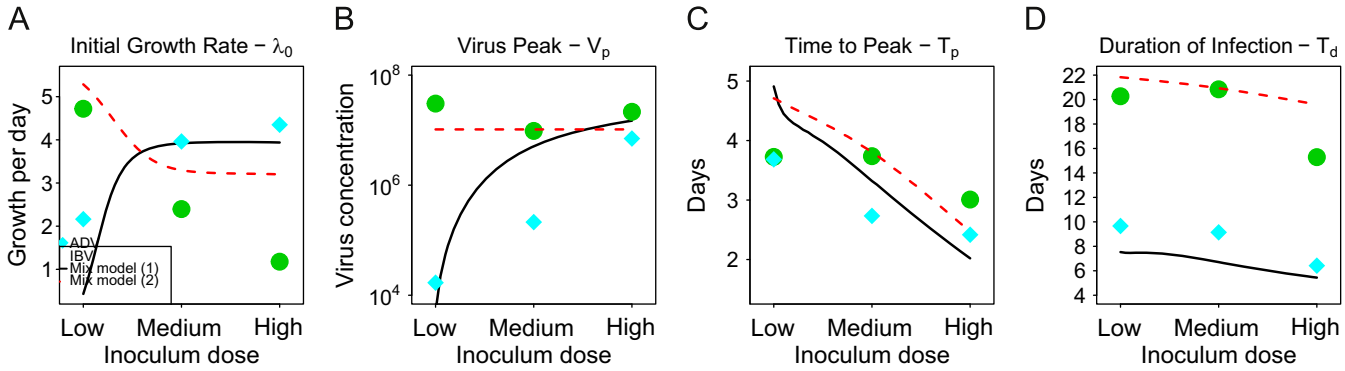

Fig. 9. Characteristic features described in Fig. 1 as a function of inoculum dose for models that combine the innate and adaptive immune response. Model 1 (solid black line) combines the cellular innate response model (M2) with the $CD8^+$ T cell model (C2). Model 2 (dashed red line) combines the cytokine innate response model (F2) with the B cell and antibody model (A1). Units of all rate parameters are inverse days, parameter values were varied until we obtained decent agreement with data. Values for model 1 are $s=10^2$, $g=10^{-5}$, $M^*=10^4$, $\delta=10$, $\alpha=10^3$, $k_M=10^{-3}$, $M_0=(sM^*)/(s+\delta)$, $r_2=1.5$, $\delta_C=1$, $s_1=1$, $k_C=1$, $C_0=1$. Values for model 2 are $g=10^3$, $\delta_2=10^2$, $k_1=2\times10^{-3}$, $k_2=1$, $F_0=1$, $f_1=1$, $r_1=0.5$, $k_B=10^{-6}$, $B_0=1$, $d=0.5$. All other parameter values as given in caption of Fig. 3. (For interpretation of the references to color in this figure caption, the reader is referred to the web version of this paper.)

Models are constantly being tested against data and modified to ensure that they can properly explain the patterns observed in the data (Saenz et al., 2010; Pawelek et al., 2012; Dobrovolny et al., 2013). Here, we studied one important pattern, namely the dependence of virus dynamics on the inoculum dose. We focused on four characteristic features that can be used to describe viral load dynamics for an acute viral infection (Smith et al., 2010; Holder and Beauchemin, 2011). We showed that while the simplest model used for acute virus infections without any immune response dynamics (assuming no changes in model parameters) can reproduce experimentally observed patterns for time to peak and duration of infection as a function of inoculum dose, the model cannot reproduce changes in the initial growth rate or virus peak. We then analyzed models that included various components of the innate and adaptive immune response. We explored how these models can or cannot reproduce aspects of the observed patterns. We found that no model for a single component of the immune response can fully capture the observed patterns, but combinations of models including innate and adaptive immune response components can.

Specifically, we found that an increase in viral load with increasing inoculum dose can be reproduced by adaptive immune response models that contain a virus (antigen) independent *growth* term. The finding that such an antigen independent component is necessary to explain the data agrees with more direct immunological studies that have shown that expansion of $CD8^+$ T cells contain an antigen independent, programmed component (Mercado et al., 2000; Wong and Pamer, 2001; van Stipdonk et al., 2001; Antia et al., 2003).

One caveat for the result that the adaptive response can influence virus peak stems from the fact that in acute infections, viral load frequently peaks after only a few days, while large numbers of B or T cells are usually only observable several days later (see e.g. Beauchemin and Handel, 2011, Fig. 1). It is still not clear how early during the infection the adaptive response becomes important. A recent review of models and data for influenza provides mixed evidence – based on only 4 studies – for the role of $CD8^+$ T cells in affecting virus peak (Dobrovolny et al., 2013, Fig. 2). We contend that for many acute viral infections, the role of the adaptive response (both T and B cells) in influencing both duration of infection and potentially viral peak is still not fully resolved. Further detailed experimental studies, possibly combined with models, are needed to address this question in more detail.

We further showed that a change in the initial growth rate can be brought about in two ways. Saturation terms, limiting the level the immune response, can lead to decreased virus growth rate as inoculum dose increases. Absorption/binding processes that lead to the initial reduction in immune response strength can lead to an increased virus growth rate as inoculum dose increases. The latter situation applies likely to situations where pre-existing adaptive immunity or high levels of innate immune effectors are present. In such a case, low levels of inoculum might not even have a positive growth rate, i.e. an infection can be prevented. However, as inoculum dose increases, the pathogen is more likely to overcome the initial level of pre-existing immunity and have a positive growth rate, leading to an infection.

We consider our study a first step toward a better understanding of the impact of inoculum dose on infection dynamics. If we could predict how changes in inoculum dose impact the immune response, especially the adaptive immune response and the generation of immune memory, it would be a significant contribution toward better vaccine design (Crotty and Ahmed, 2004; Seder, 2008; Rappuoli, 2007; Pulendran and Ahmed, 2011). In particular for live vaccines, knowing the right balance between enough inoculum to trigger a robust immune response, and low enough inoculum to prevent potential side effects is crucial (Amanna and Slifka, 2009). Similarly, for newly emerging pathogens where vaccine development is often a race against time (as for instance witnessed for the 2009 H1N1 Influenza pandemic), it is essential to optimize vaccine protection while minimizing the required vaccine dose. Current trial-and-error approaches are time-consuming and expensive. More rational ways of optimal dose determination are needed. Similarly, if we could predict the inoculum level at which an infection remains sub-lethal, and the level at which it remains sub-clinical, it could be of immense help in optimizing rules and guidelines for acceptable levels of pathogen exposure (Kothary and Babu, 2001; Julien et al., 2009; Buchanan et al., 2009).

In summary, we analyzed models for acute viral infections with regard to their ability to properly reproduce inoculum dose dependent virus dynamics. We found that only some of the existing models are suitable, and that combinations including more than one immune response component are needed to properly describe the data. The analysis presented here provides information on the types of models that are suitable, and we suggest that future models for any acute viral infection should ensure that the immune response is modeled in such a way that

inoculum dose dependent patterns can be properly reproduced. The further development of mechanistic models that can properly describe how immune response dynamics and infection outcomes depend on inoculum dose would be very valuable. The present study is a first step in that direction.

Acknowledgments

We thank the reviewers for useful and constructive feedback, which helped to improve this paper.

References

Ahmed, Rafi, Gray, David, 1996. Immunological memory and protective immunity: understanding their relation. Science 272 (April (5258)), 54–60 (ArticleType: research-article/Full publication date: April 5, 1996/Copyright 1996 American Association for the Advancement of Science).

Amanna, Ian J., Slifka, Mark K., 2009. Wanted, dead or alive: new viral vaccines. Antivir. Res. 84 (November (2)), 119–130.

Andersen, Mads Hald, Schrama, David, Straten, Per Thor, Becker, Jörgen C., 2006. Cytotoxic t cells. J. Investig. Dermatol. 126 (January (1)), 32–41.

Antia, R., Nowak, M.A., Anderson, R.M., 1996. Antigenic variation and the within-host dynamics of parasites. Proc. Natl. Acad. Sci. USA 93 (February (3)), 985–989.

Antia, Rustom, Bergstrom, Carl T., Pilyugin, Sergei S., Kaech, Susan M., Ahmed, Rafi, 2003. Models of CD8+ responses. 1. What is the antigen-independent proliferation program. J. Theor. Biol. 221 (April (4)), 585–598.

Antia, Rustom, Ganusov, Vitaly V., Ahmed, Rafi, 2005. The role of models in understanding CD8+ t-cell memory. Nat. Rev. Immunol. 5 (February (2)), 101–111.

Antia, Rustom, Koella, Jacob C., 1994. A model of non-specific immunity. J. Theor. Biol. 168 (May (2)), 141–150.

Asquith, Becca, Bangham, Charles R.M., 2003. An introduction to lymphocyte and viral dynamics: the power and limitations of mathematical analysis. Proc. Biol. Sci. 270 (August (1525)), 1651–1657, PMID: 12964991, PMCID: PMC1691432.

Baccam, Prasith, Beauchemin, Catherine, Macken, Catherine A., Hayden, Frederick G., Perelson, Alan S., 2006. Kinetics of influenza a virus infection in humans. J. Virol. 80 (August (15)), 7590–7599, WOS:000239189100030.

Beauchemin, Catherine A.A., Handel, Andreas, 2011. A review of mathematical models of influenza a infections within a host or cell culture: lessons learned and challenges ahead RID g-4619-2011. BMC Public Health 11. WOS:000290279700007.

Beauchemin, Catherine A.A., McSharry, James J., Drusano, George L., Nguyen, Jack T., Went, Gregory T., Ribeiro, Ruy M., Perelson, Alan S., 2008. Modeling amantadine treatment of influenza a virus in vitro. J. Theor. Biol. 254 (September (2)), 439–451.

Blaser, Martin J., Newman, Lee S., 1982. A review of human salmonellosis. I. Infective dose. Rev. Infect. Dis. 4 (November (6)), 1096–1106 (ArticleType: research-article/Full publication date: November–December, 1982/ Copyright 1982 Oxford University Press).

Bocharov, G.A., Romanyukha, A.A., 1994. Mathematical model of antiviral immune response. III. Influenza a virus infection. J. Theor. Biol. 167 (April (4)), 323–360.

De Boer, Rob J., 2007. Understanding the failure of CD8+ t-cell vaccination against Simian/Human immunodeficiency virus. J. Virol. 81 (March (6)), 2838–2848.

Boon, Adrianus C.M., de Beauchamp, Jennifer, Hollmann, Anna, Luke, Jennifer, Kotb, Malak, Rowe, Sarah, Finkelstein, David, Neale, Geoffrey, Lu, Lu, Williams, Robert W., Webby, Richard J., 2009. Host genetic variation affects resistance to infection with a highly pathogenic H5N1 influenza a virus in mice. J. Virol. 83 (October (20)), 10417–10426, PMID: 19706712.

Borghans, Jos A.M., De Boer, Rob J., Segel, Lee A., 1996. Extending the quasi-steady state approximation by changing variables. Bull. Math. Biol. 58 (January (1)), 43–63.

Braciale, Thomas J., Sun, Jie, Kim, Taeg S., 2012. Regulating the adaptive immune response to respiratory virus infection. Nat. Rev. Immunol. 12 (April (4)), 295–305.

Buchanan, Robert L., Havelaar, Arie H., Smith, Mary Alice, Whiting, Richard C., Julien, Elizabeth, 2009. The key events dose-response framework: its potential for application to foodborne pathogenic microorganisms. Crit. Rev. Food Sci. Nutr. 49 (8), 718–728, PMID: 19690997.

Callison, Scott A., Hilt, Deborah A., Boynton, Tye O., Sample, Brenda F., Robison, Robert, Swayne, David E., Jackwood, Mark W., 2006. Development and evaluation of a real-time taqman RT-PCR assay for the detection of infectious bronchitis virus from infected chickens. J. Virol. Methods 138 (December (1–2)), 60–65.

Canini, Laetitia, Carrat, Fabrice, 2011. Population modeling of influenza A/H1N1 virus kinetics and symptom dynamics. J. Virol. 85 (March (6)), 2764–2770, PMID: 21191031.

Cavanagh, Dave, 2007. Coronavirus avian infectious bronchitis virus. Vet. Res. 38 (2), 281–297.

Cook, Jane K.A., Jackwood, M., Jones, R.C., 2012. The long view: 40 years of infectious bronchitis research. Avian Pathol. 41 (3), 239–250.

Crotty, Shane, Ahmed, Rafi, 2004. Immunological memory in humans. Semin. Immunol. 16 (June (3)), 197–203.

De Boer, R.J., Perelson, A.S., 1998. Target cell limited and immune control models of HIV infection: a comparison. J. Theor. Biol. 190 (February (3)), 201–214.

De Boer, Rob J., Perelson, Alan S., 1994. T cell repertoires and competitive exclusion. J. Theor. Biol. 169 (August (4)), 375–390.

De Boer, Rob J., Perelson, A.S., 1995. Towards a general function describing t cell proliferation. J. Theor. Biol. 175 (August (4)), 567–576.

Dobrovolny, Hana M., Reddy, Micaela B., Kamal, Mohamed A., Rayner, Craig R., Beauchemin, Catherine A.A., 2013. Assessing mathematical models of influenza infections using features of the immune response. PLoS One 8 (February (2)), e57088.

Elemans, Marjet, Seich Al Basatena, Nafisa-Katrin, Asquith, Becca, 2012. The efficiency of the human cd8+ t cell response: how should we quantify it, what determines it, and does it matter?. PLoS Comput. Biol. 8 (2), e1002381.

Enquist, L.W., Krug, R.M., Racaniello, V.R., Skalka, A.M., Flint, S.J., Flint, S.J., 1999. Principles of virology: molecular biology, pathogenesis, and control. Am. Soc. Microbiol.

Ganusov, Vitaly V., Barber, Daniel L., De Boer, Rob J., 2011. Killing of targets by CD8 t cells in the mouse spleen follows the law of mass action. PloS One 6 (1), e15959, PMID: 21283669.

Garcia-Sastre, Adolfo, 2002. Mechanisms of inhibition of the host interferon alpha/beta-mediated antiviral responses by viruses. Microbes Infect. 4 (May (6)), 647–655.

Ginsberg, Harold S., Horsfall, Frank L., 1952. Quantitative aspects of the multiplication of influenza a virus in the mouse lung relation between the degree of viral multiplication and the extent of pneumonia. J. Exp. Med. 95 (February (2)), 135–145.

Goldberg, L.J., Watkins, H.M.S., Dolmatz, M.S., Schlamm, N.A., 1954. Studies on the experimental epidemiology of respiratory infections. VI. The relationship between dose of microorganisms and subsequent infection or death of a host. J. Infect. Dis. 94 (January (1)), 9–21 (ArticleType: research-article/Full publication date: January–February, 1954/ Copyright 1954 Oxford University Press).

Gowthaman, V., Vanamayya, P.R., Nagarajan, S., Suba, S., Bhatia, S., Jain, R., Behera, P., Tosh, C., Murugkar, H.V., Dubey, S.C., 2010. Influence of dose of inocula on outcome of clinical disease in highly pathogenic avian influenza (H5N1) infections: an experimental study. Avian Dis. 54 (March (s1)), 576–580.

Hancioglu, Baris, Swigon, David, Clermont, Gilles, 2007. A dynamical model of human immune response to influenza a virus infection. J. Theor. Biol. 246 (May (1)), 70–86.

Handel, Andreas, Antia, Rustom, 2008. A simple mathematical model helps to explain the immunodominance of CD8 t cells in influenza a virus infections. J. Virol. 82 (August (16)), 7768–7772.

Handel, Andreas, Brown, Justin, Stallknecht, David, Rohani, Pejman, 2013. A multi-scale analysis of influenza a virus fitness trade-offs due to temperature-dependent virus persistence. PLoS Comput. Biol. 9 (3), e1002989.

Handel, Andreas, Longini, Ira M., Antia, Rustom, 2010. Towards a quantitative understanding of the within-host dynamics of influenza A infections. J. R. Soc. Interface 7 (January (42)), 35–47.

Handel, Andreas, Longini , Ira M., Antia, Rustom, 2007. Neuraminidase inhibitor resistance in influenza: assessing the danger of its generation and spread. PLoS Comput. Biol. 3 (December (12)), e240.

Handel, Andreas, Margolis, Elisa, Levin, Bruce R., 2009. Exploring the role of the immune response in preventing antibiotic resistance. J. Theor. Biol. 256 (February (4)), 655–662.

Handel, Andreas, Yates, Andrew, Pilyugin, Sergei S., Antia, Rustom, 2009. Sharing the burden: antigen transport and firebreaks in immune responses. J. R. Soc. Interface 6 (May (34)), 447–454.

Harty, John T., Badovinac, Vladimir P., 2008. Shaping and reshaping cd8+ t-cell memory. Nat. Rev. Immunol. 8 (February (2)), 107–119.

Hatta, Yasuko, Hershberger, Karen, Shinya, Kyoko, Proll, Sean C., Dubielzig, Richard R., Hatta, Masato, Katze, Michael G., Kawaoka, Yoshihiro, Suresh, M., 2010. Viral replication rate regulates clinical outcome and CD8 t cell responses during highly pathogenic H5N1 influenza virus infection in mice. PLoS Pathog. 6 (October (10)), e1001139.

Heesterbeek, J.a.P., 2002. A brief history of r0 and a recipe for its calculation. Acta Biotheor. 50 (September (3)), 189–204.

Heffernan, J.M., Smith, R.J., Wahl, L.M., 2005. Perspectives on the basic reproductive ratio. J. R. Soc. Interface 2 (September (4)), 281–293.

Heffernan, J.M., Keeling, M.J., 2008. An in-host model of acute infection: measles as a case study. Theor. Popul. Biol. 73 (February (1)), 134–147.

Herold, Susanne, Steinmueller, Mirko, von Wulffen, Werner, Cakarova, Lidija, Pinto, Ruth, Pleschka, Stephan, Mack, Matthias, Kuziel, William A., Corazza, Nadia, Brunner, Thomas, Seeger, Werner, Lohmeyer, Juergen, 2008. Lung epithelial apoptosis in influenza virus pneumonia: the role of macrophage-expressed tnf-related apoptosis-inducing ligand. J. Exp. Med. 205 (December (13)), 3065–3077.

Höegner, Katrin, Wolff, Thorsten, Pleschka, Stephan, Plog, Stephanie, Gruber, Achim D., Kalinke, Ulrich, Walmrath, Hans-Dieter, Bodner, Johannes, Gattenlohner, Stefan, Lewe-Schlosser, Peter, Matrosovich, Mikhail, Seeger, Werner, Lohmeyer, Juergen, Herold, Susanne, 2013. Macrophage-expressed IFN-β contributes to apoptotic alveolar epithelial cell injury in severe influenza virus pneumonia. PLoS Pathog. 9 (February (2)), e1003188.

Holder, Benjamin P., Beauchemin, Catherine A.A., 2011. Exploring the effect of biological delays in kinetic models of influenza within a host or cell culture RID g-4619-2011. BMC Public Health 11, WOS:000290279700010.

Howey, Richard, Quan, Melvyn, Savill, Nicholas J., Matthews, Louise, Alexandersen, Soren, Woolhouse, Mark, 2009. Effect of the initial dose of foot-and-mouth disease virus on the early viral dynamics within pigs. J. R. Soc. Interface 6 (October (39)), 835–847.

Hughes, G.J., Kitching, R.P., Woolhouse, M.E.J., 2002. Dose-dependent responses of sheep inoculated intranasally with a type o foot-and-mouth disease virus. J. Comp. Pathol. 127 (July (1)), 22–29.

Julien, Elizabeth, Boobis, Alan R., Olin, Stephen S., The ILSI Research Foundation Threshold Working Group, 2009. The key events dose-response framework: a cross-disciplinary mode-of-action based approach to examining dose-response and thresholds. Crit. Rev. Food Sci. Nutr. 49(8), 682–689. PMID: 19690994.

Kaech, S.M., Ahmed, R., 2001. Memory CD8+ t cell differentiation: initial antigen encounter triggers a developmental program in naïve cells. Nat. Immunol. 2 (May (5)), 415–422.

Kochin, Beth F., Yates, Andrew J., de Roode, Jacobus C., Antia, Rustom, 2010. On the control of acute rodent malaria infections by innate immunity. PLoS One 5 (May (5)), e10444.

Kothary, Mahendra H., Babu, Uma S., 2001. Infective dose of foodborne pathogens in volunteers: a review. J. Food Saf. 21 (1), 49–68.

La Gruta, Nicole L., Kedzierska, Katherine, Stambas, John, Doherty, Peter C., 2007. A question of self-preservation: immunopathology in influenza virus infection. Immunol. Cell Biol. 85 (February (2)), 85–92.

Lee, Ha Youn, Topham, David J., Park, Sung Yong, Hollenbaugh, Joseph, Treanor, John, Mosmann, Tim R., Jin, Xia, Ward, Brian M., Miao, Hongyu, Holden-Wiltse, Jeanne, Perelson, Alan S., Zand, Martin, Wu, Hulin, 2008. Simulation and prediction of the adaptive immune response to influenza a virus infection. J. Virol. 83 (July (14)), 7151–7165.

Legge, Kevin L., Braciale, Thomas J., 2005. Lymph node dendritic cells control CD8+ t cell responses through regulated FasL expression. Immunity 23 (December (6)), 649–659.

Leggett, Helen C., Cornwallis, Charlie K., West, Stuart A., 2012. Mechanisms of pathogenesis, infective dose and virulence in human parasites. PLoS Pathog. 8 (February (2)), e1002512.

Liu, Guangliang, Kahan, Shannon M., Jia, Yali, Karst, Stephanie M., 2009. Primary High-Dose murine norovirus 1 infection fails to protect from secondary challenge with homologous virus. J. Virol. 83 (July (13)), 6963–6968.

Marois, Isabelle, Cloutier, Alexandre, Garneau, Émilie, Richter, Martin V., 2012. Initial infectious dose dictates the innate, adaptive, and memory responses to influenza in the respiratory tract. J. Leukoc. Biol. 92 (July (1)), 107–121.

Mercado, Roberto, Vijh, Sujata, Elise Allen, S., Kerksiek, Kristen, Pilip, Ingrid M., Pamer, Eric G., 2000. Early programming of t cell populations responding to bacterial infection. J. Immunol. 165 (December (12)), 6833–6839.

Mitchell, Hugh, Levin, Drew, Forrest, Stephanie, Beauchemin, Catherine A.A., Tipper, Jennifer, Knight, Jennifer, Donart, Nathaniel, Colby Layton, R., Pyles, John, Gao, Peng, Harrod, Kevin S., Perelson, Alan S., Koster, Frederick, 2011. Higher level of replication efficiency of 2009 (H1N1) pandemic influenza virus than those of seasonal and avian strains: kinetics from epithelial cell culture and computational modeling. J. Virol. 85 (January (2)), 1125–1135, PMID: 21068247.

Moskophidis, D., Battegay, M., van den Broek, M., Laine, E., Hoffmann-Rohrer, U., Zinkernagel, R.M., 1995. Role of virus and host variables in virus persistence or immunopathological disease caused by a non-cytolytic virus. J. Gen. Virol. 76 (February (Pt 2)), 381–391.

Murphy, Kenneth M., 2012. Janeway's Immunobiology, 8th ed. Garland Science

Nazir, Shoab A., Metcalf, Jordan P., 2005. Innate immune response to adenovirus. J. Investig. Med. 53 (September (6)), 292–304.

Nowak, M.A., Lloyd, A.L., Vasquez, G.M., Wiltrout, T.A., Wahl, L.M., Bischofberger, N., Williams, J., Kinter, A., Fauci, A.S., Hirsch, V.M., Lifson, J.D., 1997. Viral dynamics of primary viremia and antiretroviral therapy in simian immunodeficiency virus infection. J. Virol. 71 (October (10)), 7518–7525, PMID: 9311831.

Nowak, Martin, May, Robert M., 2000. Virus Dynamics: Mathematical Principles of Immunology and Virology. Oxford University Press, November

Ottolini, Martin G., Blanco, Jorge C.G., Eichelberger, Maryna C., Porter, David D., Pletneva, Lioubov, Richardson, Joann Y., Prince, Gregory A., 2005. The cotton rat provides a useful small-animal model for the study of influenza virus pathogenesis. J. Gen. Virol. 86 (October (10)), 2823–2830.

Ottolini, Martin G., Porter, David D., Hemming, Val G., Hensen, Sally A., Sami, Iman R., Prince, Gregory A., 1996. Semi-permissive replication and functional aspects of the immune response in a cotton rat model of human parainfluenza virus type 3 infection. J. Gen. Virol. 77 (August (8)), 1739–1743.

Pawelek, Kasia A., Huynh, Giao T., Quinlivan, Michelle, Cullinane, Ann, Rong, Libin, Perelson, Alan S., 2012. Modeling within-host dynamics of influenza virus infection including immune responses. PLoS Comput. Biol. 8 (June (6)), 1–13.

Perelson, Alan S., 2002. Modelling viral and immune system dynamics. Nat. Rev. Immunol. 2 (January (1)), 28–36.

Perelson, Alan S., Mirmirani, Majdedin, Oster, George F., 1976. Optimal strategies in immunology. J. Math. Biol. 3 (September (3–4)), 325–367.

Pilyugin, Sergei S., Antia, Rustom, 2000. Modeling immune responses with handling time. Bull. Math. Biol. 62 (September (5)), 869–890.

Powell, Timothy J., Dwyer, David W., Morgan, Tammy, Hollenbaugh, Joseph A., Dutton, Richard W., 2006. The immune system provides a strong response to even a low exposure to virus. Clin. Immunol. 119 (April (1)), 87–94.

Prince, G.A., Porter, D.D., Jenson, A.B., Horswood, R.L., Chanock, R.M., Ginsberg, H.S., 1993. Pathogenesis of adenovirus type 5 pneumonia in cotton rats (*Sigmodon hispidus*). J. Virol. 67 (January (1)), 101–111.

Pulendran, Bali, Ahmed, Rafi, 2011. Immunological mechanisms of vaccination. Nat. Immunol. 12 (6), 509–517.

Quan, M., Murphy, C.M., Zhang, Z., Alexandersen, S., 2004. Determinants of early foot-and-mouth disease virus dynamics in pigs. J. Comp. Pathol. 131 (November (4)), 294–307.

Rappuoli, R., 2007. Bridging the knowledge gaps in vaccine design. Nat. Biotechnol. 25 (December (12)), 1361–1366.

R Development Core Team, 2012. R: A Language and Environment for Statistical Computing. R Foundation for Statistical Computing, Vienna, Austria. ISBN 3-900051-07-0.

Randall, Richard E., Goodbourn, Stephen, 2008. Interferons and viruses: an interplay between induction signalling antiviral responses and virus countermeasures. J. Gen. Virol. 89 (January (1)), 1–47.

Regoes, Roland R., Barber, Daniel L., Ahmed, Rafi, Antia, Rustom, 2007a. Estimation of the rate of killing by cytotoxic t lymphocytes in vivo. Proc. Natl. Acad. Sci. 104 (January (5)), 1599–1603.

Regoes, Roland R., Yates, Andrew, Antia, Rustom, 2007b. Mathematical models of cytotoxic t-lymphocyte killing. Immunol. Cell Biol. 85 (June (4)), 274–279.

Reperant, Leslie A., Kuiken, Thijs, Grenfell, Bryan T., Osterhaus, Albert D.M.E., Dobson, Andrew P., 2012. Linking influenza virus tissue tropism to population-level reproductive fitness. PLoS One 7 (August (8)), e43115.

Saenz, Roberto A., Quinlivan, Michelle, Elton, Debra, Mac Rae, Shona, Blunden, Anthony S., Mumford, Jennifer A., Daly, Janet M., Digard, Paul, Cullinane, Ann, Grenfell, Bryan T., McCauley, John W., Wood, James L.N., Gog, Julia R., 2010. Dynamics of influenza virus infection and pathology. J. Virol. 84 (April (8)), 3974–3983.

Schmid-Hempel, Paul, Frank, Steven A., 2007. Pathogenesis, virulence, and infective dose. PLoS Pathog. 3 (October (10)), e147.

Seder, Robert A., Darrah, P.A., Roederer, M., 2008. T-cell quality in memory and protection: implications for vaccine design. Nat. Rev. Immunol. 8 (June (6)), 486.

Segel, Lee A., Slemrod, Marshall, 1989. The quasi-steady-state assumption: a case study in perturbation. SIAM Rev. 31 (September (3)), 446–477 (ArticleType: research-article/Full publication date: September, 1989/Copyright 1989 Society for Industrial and Applied Mathematics).

Smith, Amber M., Adler, Frederick R., Perelson, Alan S., 2010. An accurate two-phase approximate solution to an acute viral infection model. J. Math. Biol. 60 (May (5)), 711–726.

Smith, Amber M., McCullers, Jonathan A., Adler, Frederick R., 2011. Mathematical model of a three-stage innate immune response to a pneumococcal lung infection. J. Theor. Biol. 276 (May (1)), 106–116.

Smith, Amber M., Perelson, Alan S., 2011. Influenza a virus infection kinetics: quantitative data and models. Wiley Interdiscipl. Rev.: Syst. Biol. Med. 3 (July (4)), 429–445.

Steinmeyer, Shelby H., Wilke, Claus O., Pepin, Kim M., 2010. Methods of modelling viral disease dynamics across the within- and between-host scales: the impact of virus dose on host population immunity. Philos. Trans. R. Soc. Lond. B: Biol. Sci. 365 (June (1548)), 1931–1941.

Tamura, S.I., Kurata, T., 2004. Defense mechanisms against influenza virus infection in the respiratory tract mucosa. Jpn. J. Infect. Dis. 57 (December (6)), 236–247.

van Stipdonk, M.J., Lemmens, E.E., Schoenberger, S.P., 2001. Naïve CTLs require a single brief period of antigenic stimulation for clonal expansion and differentiation. Nat. Immunol. 2 (May (5)), 423–429.

Vickers, David M., Zhang, Qian, Osgood, Nathaniel D., 2009. Immunobiological outcomes of repeated chlamydial infection from two models of within-host population dynamics. PLoS One 4 (9), e6886, PMID: 19727394.

Welsh, Raymond M., Bahl, Kapil, Marshall, Heather D., Urban, Stina L., 2012. Type 1 interferons and antiviral cd8 t-cell responses. PLoS Pathog. 8 (January (1)), e1002352.

Wodarz, Dominik, 2007. Killer Cell Dynamics: Mathematical and Computational Approaches to Immunology, vol. 32. Springer, New York http://amzn.com/0387308938.

Wong, Phillip, Pamer, Eric G., 2001. Cutting edge: antigen-independent CD8 t cell proliferation. J. Immunol. 166 (May (10)), 5864–5868.

Yate, Andrew, Graw, Frederik, Barber, Daniel L., Ahmed, Rafi, Regoes, Roland R., Antia, Rustom, 2007. Revisiting estimates of CTL killing rates in vivo. PLoS One 2 (December (12)), e1301.

Yates, Andrew J., Van Baalen, Minus, Antia, Rustom, 2011. Virus replication strategies and the critical CTL numbers required for the control of infection. PLoS Comput. Biol. 7 (November (11)), e1002274.

Yewdell, Jonathan W., 2010. Designing cd8+ t cell vaccines: it's not rocket science (yet). Curr. Opin. Immunol. 22 (June (3)), 402–410.